SECOND EUROPEAN ROTORCRAFT AND POWERED LIFT FORUM

Paper No 20

TRAILING VORTEX WAKE STRUCTURE

R G Sampson

Royal Military College of Science
Shrivenham, England

September 20-22 1976

Bückeburg, Federal Republic of Germany

Deutsche Gesellschaft für Luft - und Raumfarht e.V.

Postfach 510645, D - 5000 Köln, Germany

TRAILING VORTEX WAKE STRUCTURE

by

R G Sampson

Royal Military College of Science

SUMMARY

The wake trailed by a half-wing mounted in an open-jet wind tunnel has been studied over a transverse plane five chords downstream. Vorticity contours show a well defined tip vortex, together with a diffuse vortex sheet which contains a significant portion of the circulation.

Calculations of the roll-up of a sheet of line vortices is shown to represent the shape of the experimental vorticity contours, and the tip vortex strength, very well. In addition, the velocity distribution within the tip vortex is shown to compare well with a logarithmic circulation distribution for a turbulent line vortex.

1. INTRODUCTION

In most flight regimes of a helicopter the tip vortex trailed from one blade passes close to the following blade. Eg, Fig 1 shows a smoke flow visualisation study of a two bladed rotor at the Royal Military College of Science (RMCS). As one blade passes the smoke injection plane the tip vortex from the previous blade is less than one chord from the blade[1].

The close passage of the vortex produces large spanwise variations in loading. The loading distribution is not, of course, predicted by conventional blade-element momentum theory and although various wake models are in use to account for the presence of the tip vortices recent work has shown that the problem is still not adequately understood[2,3]. Evaluating the AGARD meeting on the Aerodynamics of Rotary Wings at Marseilles in 1972 Ham[2] pointed out that better understanding is required of the tip vortex formation process, the tip vortex structure, the rolling up of the blade trailing wake and the interaction between the tip vortex and blade. Ham concluded that this is necessary before a satisfactory method of rotor wake geometry prediction can be achieved.

More information on some of these phenomena is provided by the results of an investigation at RMCS in which the vortex wake trailed by a half-wing has been studied by traversing a five-hole yaw probe over a transverse plane of the flow. The velocity measurements have allowed the structure of the tip vortex and vortex sheet to be defined and this is shown to agree well with the calculated roll-up of a sheet of line vortices. The tip vortex is shown to be well represented by a turbulent line vortex model.

2. EXPERIMENTAL SET-UP

The tests were carried out in the Open Jet Wind Tunnel at RMCS[4]. This tunnel has an elliptical working section with major and minor axes of 1.5 m and 1.1 m respectively. A 55 kW electric motor driving the fan through a hydrostatic transmission provides a maximum working section velocity of 42 m/s. The velocity used in these tests was 30 m/s, at which the turbulence level in the tunnel is 0.75%.

The wakes to be studied were generated by a 0.175 chord, 0.5 m semispan half-wing of NACA 0012 section, mounted vertically on a reflection plate projecting from the tunnel nozzle. Fig 2 shows the tunnel working section with the half-wing in position. Measurements were made with the wing at incidences of 3^o, 6^o and 12^o. The more complete results for 3^o and 12^o are presented here.

Measurements were made in a transverse plane five chords downstream of the wing trailing edge using a five hole yaw probe (Fig 3). The probe was made as small as practicable to minimise interference effects - the sensing tubes were of 0.9 mm outside diameter. The probe was mounted in a traverse gear which allowed a vertical traverse from one chord above the wing tip to one chord below (ie in the spanwise sense). Between runs the probe could be moved to different horizontal positions. In this way an area of approximately 2 chords x $1\frac{1}{2}$ chords was surveyed. When in use the probe was rotated in pitch to balance the pressures sensed by the top and bottom tubes. Reference to calibration curves then permitted pitch and yaw angles, static and total pressure and absolute velocity to be determined.

3. EXPERIMENTAL RESULTS

Fig 4 shows distribution of non-dimensionalised downwash and sidewash velocities, obtained from spanwise traverses close to the tip vortex centre, for the wing at 3^o and 12^o incidence. (Although the half-wing was mounted vertically the results are presented throughout in the conventional sense relating to a horizontal lifting surface). As expected, the downwash rises with decreasing distance from the vortex centre, peaks and then fall almost linearly through the vortex core. The larger values for the wing at 12^o are clearly evident. The sidewash is close to zero with small values occurring close to the vortex centre. Results from traverses further from the vortex centre showed that the downwash values were reduced, whilst the sidewash velocities reached higher values.

Velocity data such as shown in Fig 4 was obtained for over twenty spanwise traverses at each wing incidence. In this way the velocity variations normal to the span were accurately defined eg Fig 5. The availability of velocity data over an area then allows the distribution of vorticity to be calculated. Streamwise vorticity ξ is given in non-dimensional form by

$$\frac{c\xi}{U_\infty} = \frac{\partial(w/U_\infty)}{\partial(y/c)} - \frac{\partial(v/U_\infty)}{\partial(z/c)}$$

and is readily determined at a point by taking the slopes of spanwise and normal velocity curves passing through that point.

Vorticity contours are shown in Figs 6 and 7 for the wing at 3^o and 12^o incidence respectively. Both figures show a well-defined tip vortex and a diffuse vortex sheet stretching in a spanwise direction. For 3^o the centre of the tip vortex has moved inboard of the wing tip and is almost in the plane of the wing. The vortex sheet has moved below the wing under the influence of the tip vortex, its image and the wing bound vorticity. For 12^o the larger circulations have resulted in the sheet movement being greater, and the tip vortex moving well below the wing plane and further inboard. Vorticity rises towards the tip vortex centre and the peak values are roughly proportional to lift coefficient. It is interesting to note a region of low vorticity entrained in the 12^o vortex as roll-up has proceeded.

The vorticity levels in the vortex sheet are low; however, the sheet cannot be considered insignificant. For 3^o incidence the sheet contributes approximately 30% of the circulation found in the measurement plane. At 12^o incidence the sheet contribution drops to approximately 10%, but further vorticity would be found further inboard than the measurement plane. Further downstream the sheet may be expected to roll-up into the tip vortex and raise its strength.

4. COMPARISON WITH PREVIOUS EXPERIMENTAL WORK

The results presented here throw new light on some previous experimental studies of tip vortices.

McCormick et al[5] used a vorticity meter in which the rotational speed of a pair of straight-crossed vanes was measured. From surveys, over transverse planes, with this meter they deduced that roll-up of the tip vortex was complete four chords downstream of a rectangular wing. However, this type of meter is insensitive to the levels of vorticity pertaining in the vortex sheet shown here, eg the non-dimensional values 0.1 and 0.2 correspond to rotational speeds of 8.5 rad/s and 17 rad/s respectively. Significant contributions from the sheet may thus be overlooked when using this type of instrumentation.

Other experimental studies of trailing vortex wake structure have in general relied on a single traverse through the vortex centre to obtain tangential velocities. The vortex wake has therefore been assumed to be rolled up into a discrete vortex and this has resulted in discrepancies between expected and measured tip vortex strengths.

Eg from hot-wire anemometer studies of the tip vortex trailed from a single Wessex rotor blade Cook[6] found measured tip vortex strengths well below the expected values. Although the results suggested that the tip vortex strength was not changing with time from generation it is likely that a significant portion of the trailed vorticity was still contained in a vortex sheet.

Rorke and Moffitt[7] also used single traverses, parallel and normal to the span, in a study of tip vortices generated by a rectangular wing tip and a 'reverse ogee' tip shown in Fig 8. The spanwise extent of the traverse is also shown: traverses were made two and five chord downstream of the wings. Although the lift coefficient of the ogee tip was found to be slightly higher than that of the rectangular tip at all incidences the maximum tangential velocity found for the ogee tip was approximately 25% of that found for the rectangular wing at the same angle of attack. However, significant vorticity may exist inboard of the reverse ogee and without a comprehensive study of the vorticity structure, such as presented here, no firm conclusions as to the benefits of the ogee tip can be drawn.

5. COMPARISON WITH A THEORETICAL MODEL OF VORTEX SHEET ROLL-UP

A method commonly adopted for calculating the development of trailing vorticity downstream of a lifting surface is to replace the vortex sheet by a distribution of line vortices and calculate the time-wise development, (Fig 9). Such an approach was first used by Westwater[8] in 1935, but as pointed out by Donaldson and Bilanin in a recent AGARDograph[9] on vortex wakes, the question of whether the roll-up phenomenon is modelled accurately in this way, or whether the calculation merely looks correct, has still to be resolved. The vorticity data of Figs 6 and 7 provides an opportunity for determining the validity of the Westwater type model.

Initial attempts were made using ten vortices per semispan as used by Westwater; ie equal strength vortices distributed in accordance with elliptic loading. (The actual wing loading was not known, but it was considered that elliptic loading would be representative). Some problems were encountered in getting the numerical model to perform phenomenologically; large timesteps resulted in excessive filament movements, particularly where the filaments were close together; reducing the timesteps resulted in the sheet appearing to cross itself. After experimenting with various combinations 25 line vortices over each semispan were used together with the following steps:

0.01 chord steps from trailing edge to 0.2 chords downstream
then 0.1 chord steps to 1 chord downstream
then 0.5 chord steps to 5 chords downstream

Timewise development of the sheet roll-up is related to downstream spacial development by replacing time by x/U_∞ .

The results of these calculations are shown in Fig 10 for 3° incidence and Fig 11 for 12° incidence, compared in each case with the experimental results. The calculations represent the shape of the experimental contours very well: the variations in size of the tip vortex and the relative positions of the vortex sheet are well predicted. Comparing the axes of the theoretical and experimental results shows, however, that the theoretical model over-predicts the inboard movement of the tip vortex and under-predicts the downward movement of the vortex and sheet. These discrepancies may be attributed to: three dimensionality of the real vortex sheet; absence of wing bound vorticity in the theoretical model; and image effects.

The line vortex model implies infinite vorticity, concentrated in infinitesimal areas whereas the measurements in the tunnel give a continuous distribution of finite vorticity over a finite area. On a vorticity basis there is thus difficulty in comparing the two sets of results on other than a qualitative pictorial basis as in Figs 10 and 11. It is possible, however, to compare the strength of the vortex filaments rolled up in the tip region of the theoretical model with the actual circulation of the tip vortex taken alone, and satisfactory agreement is obtained:

Incidence	No of filaments in tip vortex	Equivalent circulation	Actual circulation
3°	11	$0.37\ m^2/s$	$0.40\ m^2/s$
12°	14	$1.90\ m^2/s$	$1.69\ m^2/s$

Further comparison between theory and experiment must be made on the basis of induced velocities, and typical results for traverses outside the tip vortex are shown in Fig 12. To make the comparison more realistic the theoretical vortex sheet has been shifted so that the centre of the tip spiral coincides with the experimental vortex centre. The agreement on downwash w/U_∞ is seen to be quite good. For sidewash v/U_∞ the line vortex model predicts values which are too high, especially at the inboard end of the traverse. This indicates that the actual strength of the vortex sheet is less than the theoretical, probably due to viscous dissipation of the vorticity. The strength of a fully rolled up vortex will therefore be less than would be expected from an inviscid model, because some of the vorticity in the vortex sheet will be dissipated before roll-up is complete.

6. COMPARISON WITH THEORETICAL TIP VORTEX MODELS

Within the spiral at the end of the line vortex model valid comparison with the experimental results is not possible because of the jumps in velocity which occur as successive turns of the spiral are crossed: a theoretical model for an isolated vortex is more appropriate.

The velocity distribution through the tip vortex suggests the classical Rankine vortex form of a free vortex with a forced vortex core. However, attempts to match a Rankine vortex to the measured velocity distributions resulted in either the peak velocity or core size being over estimated by a factor of two. A similar result was found by Cook[6] in his rotor blade tip vortex measurements. The laminar viscous vortex model[10], in which viscosity rounds off the tangential velocity peak, was also found unsatisfactory. An eddy viscosity must be introduced to match the model to the vortices described here, but agreement could only be achieved by varying the eddy viscosity with radius.

The most appropriate model for the present case is the turbulent vortex model of Hoffman and Joubert[11]. By an elegant extension of the mixing length concept they derived the circulation distribution as logarithmic:

$$\frac{\Gamma}{\Gamma_1} = A \log_{10}\left(\frac{r}{r_1}\right) + 1$$

Γ_1 is analogous to friction velocity in boundary layer terms, and is chosen to be the circulation at radius r_1 where peak tangential velocity occurs. Based on wind tunnel tests Hoffman and Joubert suggested a value of 2.14 for the slope A.

Fig 13 compares the mean circulation distribution for the 3° and 12° vortices with Hoffman and Jouberts model. Over the range for which the logarithmic profile pertains excellent agreement occurs, confirming the choice of $A = 2.14$. Near the centre of the vortices is an inner 'eye' of solid body rotation, and the circulation distribution here is best described by

$$\frac{\Gamma}{\Gamma_1} = 1.47\left(\frac{r}{r_1}\right)^2$$

Beyond $r/r_1 = 2$ the circulation falls away from the logarithmic distribution - this is symptomatic of the assymetry caused by incomplete roll-up of the vortex sheet.

In Fig 14 velocity distributions for traverses through the tip vortex centre are compared with Hoffman and Joubert within the tip vortex, and the line vortex model outside. For the 12° incidence results the velocity peaks are under-estimated, and the velocity is over-estimated outboard of the wing tip. However the combination of the two models provides a reasonable basis for the downwash prediction.

7. CONCLUSIONS

Significant amounts of vorticity are to be found in the non-rolled-up vortex sheet several chords downstream of a lifting surface, although a well-defined and approximately axisymmetric tip vortex exists. A line vortex model for calculating vortex sheet roll-up gives results which are close to those observed experimentally. The turbulent line vortex model of Hoffman and Joubert predicts the structure of the tip vortex extremely well and the use of 2.14 for the slope of the logarithmic circulation distribution is supported by the resulted presented here.

8. ACKNOWLEDGEMENTS

The Author would like to thank RMCS for permission to publish this work, and Messrs J Pryor and P Foley of the Mechanical Engineering Department RMCS for assistance with the experimental investigation.

9. REFERENCES

1. R H Midwinter and A R Philp, Rotor Wakes at the Hover
   RMCS 28 Degree Project Report May 1976

2. N D Ham, Technical Evaluation Report on Fluid Dynamics Panel Specialists Meeting on Aerodynamics of Rotary Wings.
   AGARD-AR-61 March 1973

3. R A Ormiston, Comparison of Several Methods for Predicting Loads on a Hypothetical Helicopter Rotor. AHS/NASA-Ames Specialist Meeting on Rotorcraft Dynamics, California, Feb 13th-15th 1974
   Also: Jnl AHS Vol 19 No 4 Oct 1974

4. K D J Ross and R G Sampson, The RMCS 5 ft x 3.75 ft Open Jet Wind Tunnel. Design and Calibration. RMCS Report/1/74 March 1974

5. B W McCormick, J L Tangler and K E Sherrieb, Structure of Trailing Vortices. AIAA J Aircraft Vol 5 No 3 May-June 1968

6. C V Cook, The Structure of the Rotor Blade Tip Vortex. Paper 3 The Aerodynamics of Rotary Wings. AGARD CP111 Feb 1973

7. J B Rorke and R C Moffitt, Wind Tunnel Simulation of Full Scale Vortices. NASA CR-2180 March 1973

8. F L Westwater, The Rolling Up of the Surface of Discontinuity Behind an Aerofoil of Finite Span, ARC R and M 1692 Aug 1935

9. C du P Donaldson and A J Bilanin, Vortex Wakes of Conventional Aircraft, AGARDograph No 204 May 1975

10. B G Newman, Flow in a Viscous Trailing Vortex, The Aeronautical Quarterly, Vol 10 May 1959

11. E R Hoffman and P N Joubert, Turbulent Line Vortices.
    J Fluid Mech (1963) Vol 16 Pt 3

10. LIST OF SYMBOLS

A	slope of logarithmic circulation distribution
c	wing chord
r	radius
r_1	radius at which peak tangential velocity occurs in tip vortex
u,v,w	velocity components in x,y,z directions respectively
U_∞	free stream velocity
x,y,z	right handed coordinates, origin at wing tip trailing edge at zero incidence: x positive in stream direction: y positive inboard
Γ	circulation
Γ_1	circulation at radius for peak velocity
ξ	vorticity component in the x-direction

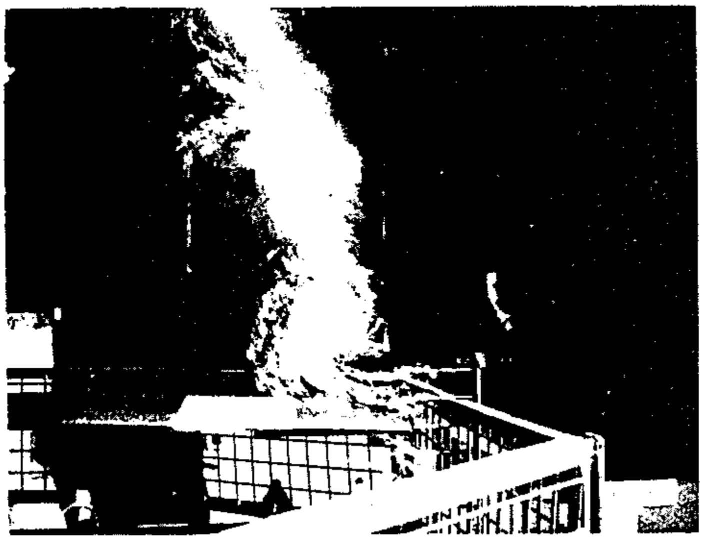

Fig 1 Tip vortices from a Two-Bladed Rotor

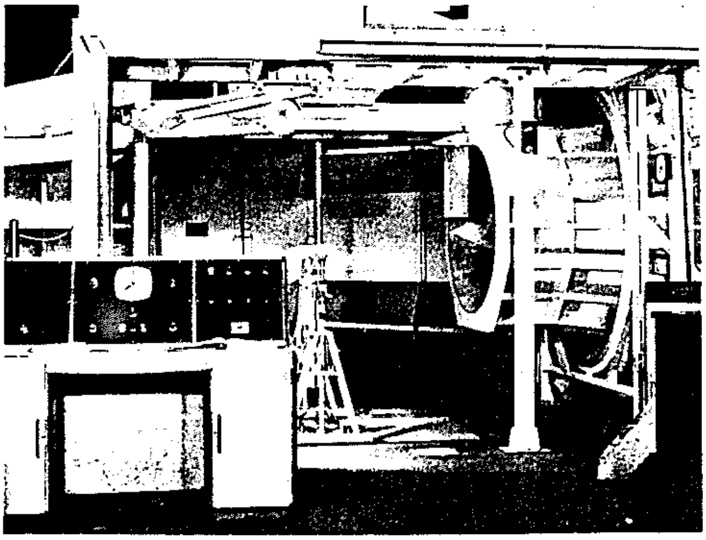

Fig 2 Half-wing Mounted in RMCS Open Jet Tunnel

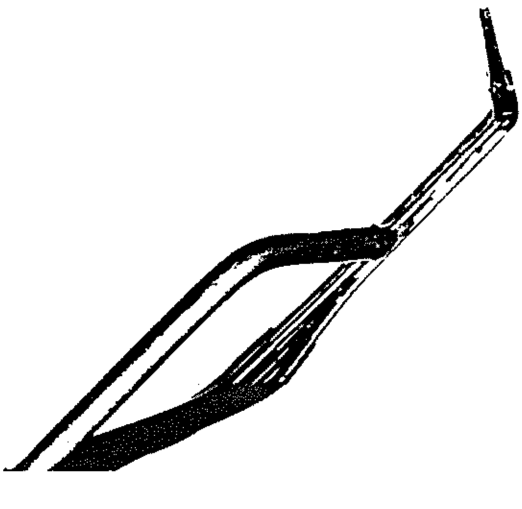

Fig 3 Five-hole Yaw Probe

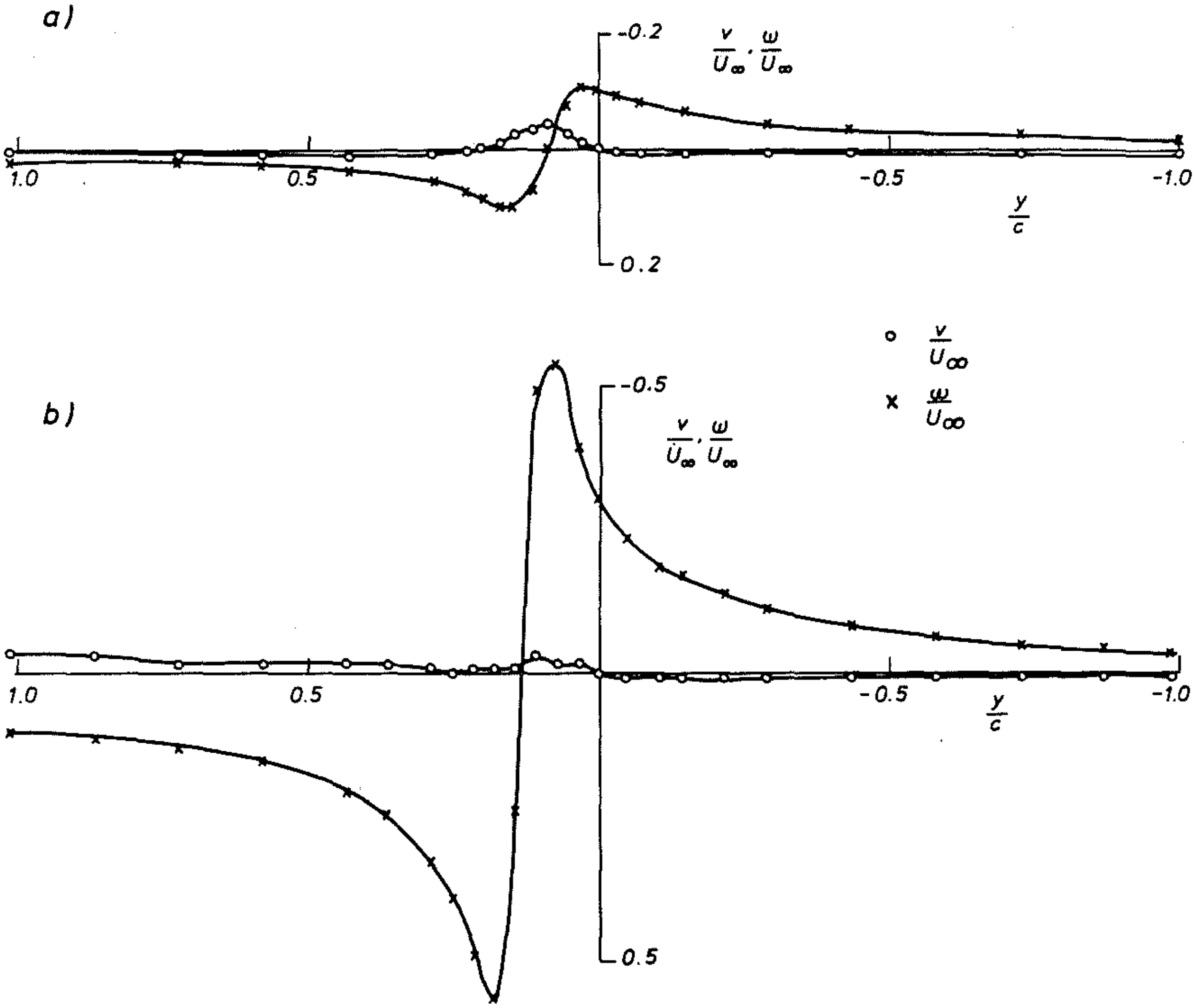

Fig 4 Velocity distributions for traverses through vortex centre
$x/c = 5.0$
a) 3^{o} incidence, $z/c = -0.006$
b) 12^{o} incidence, $z/c = 0.237$

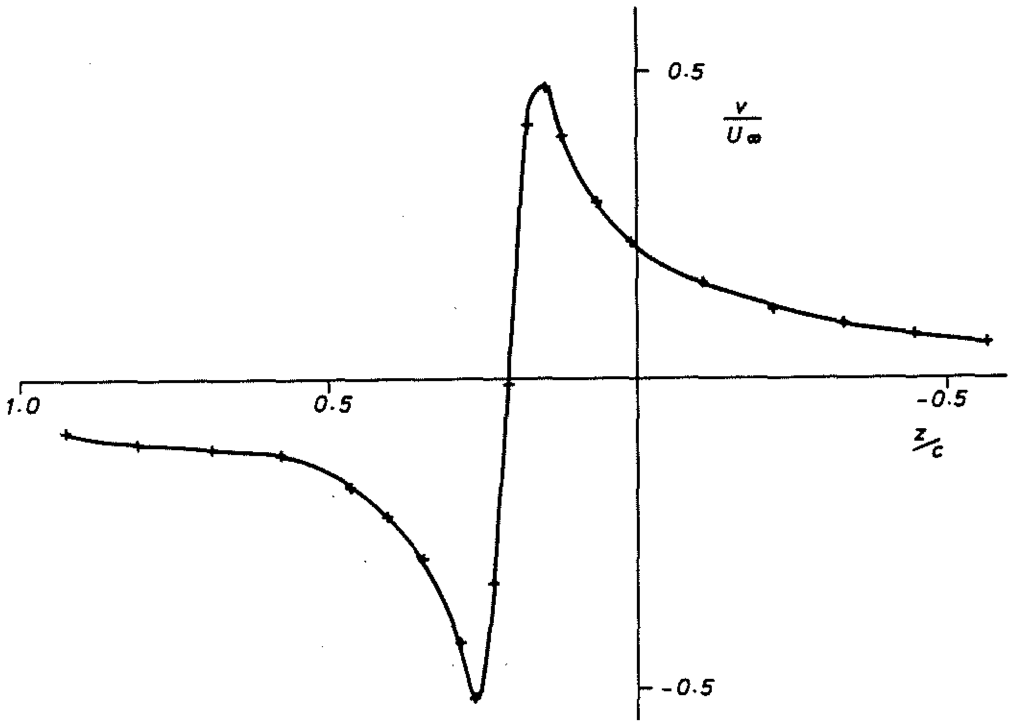

Fig 5 Velocity distribution normal to span
$x/c = 5.0$ 12^{o} incidence $y/c = 0.145$

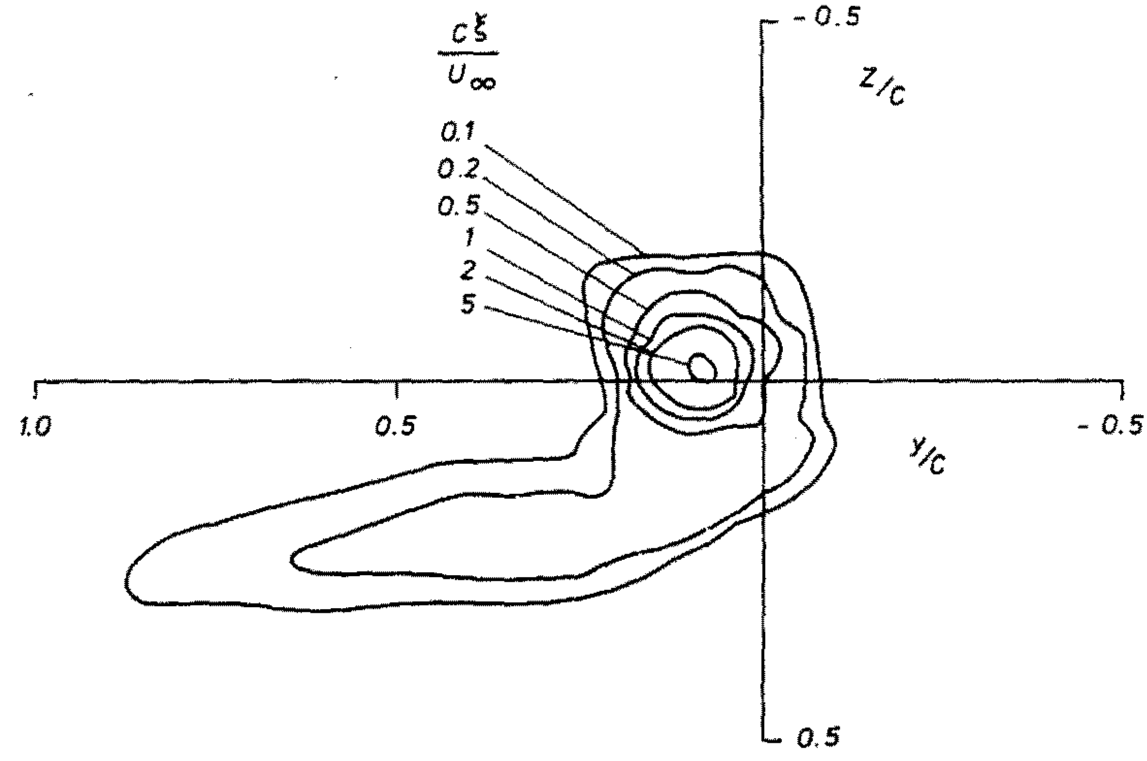

Fig 6 Vorticity contours x/c = 5.0 3° incidence

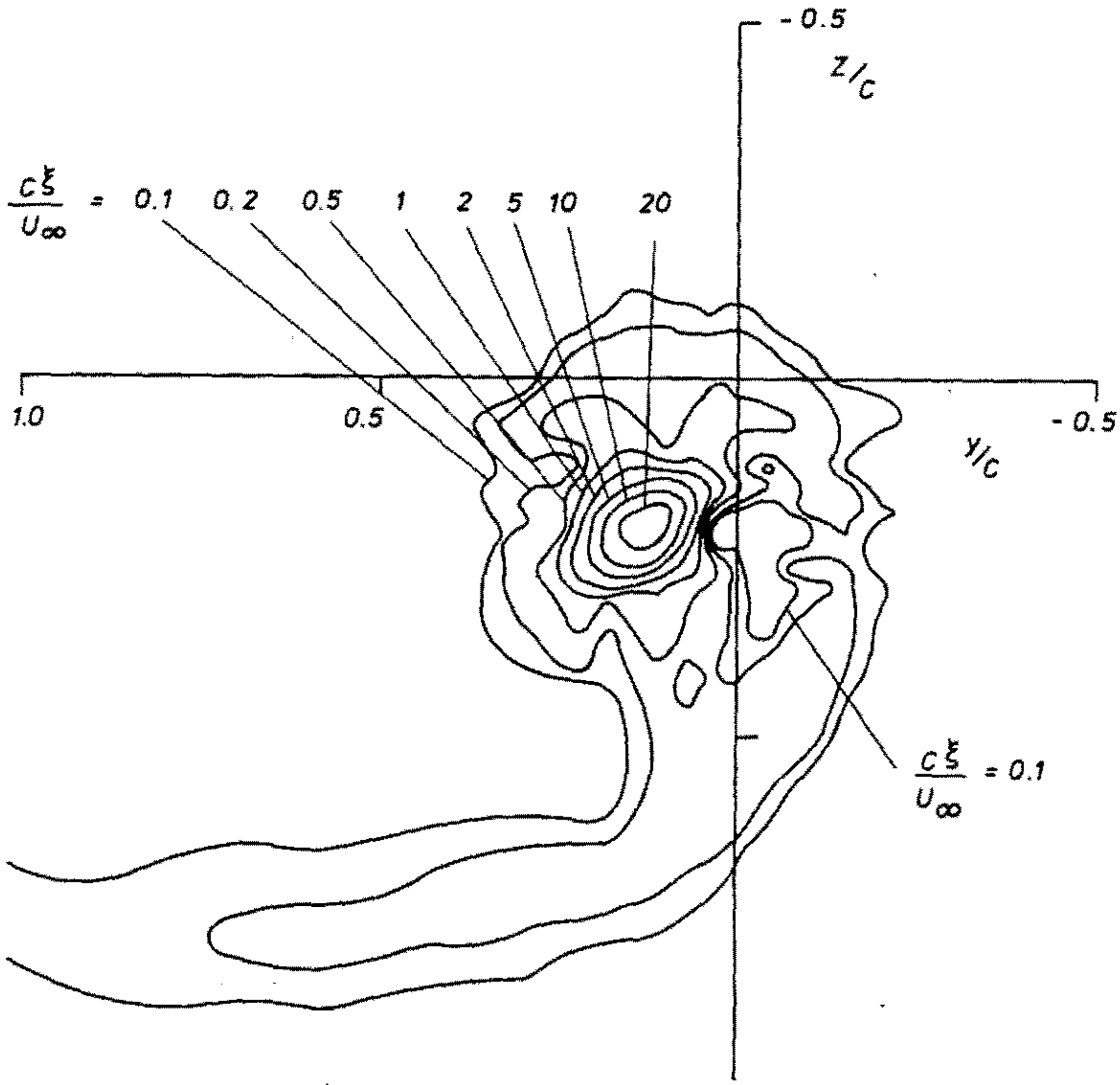

Fig 7 Vorticity contours x/c = 5.0 12° incidence

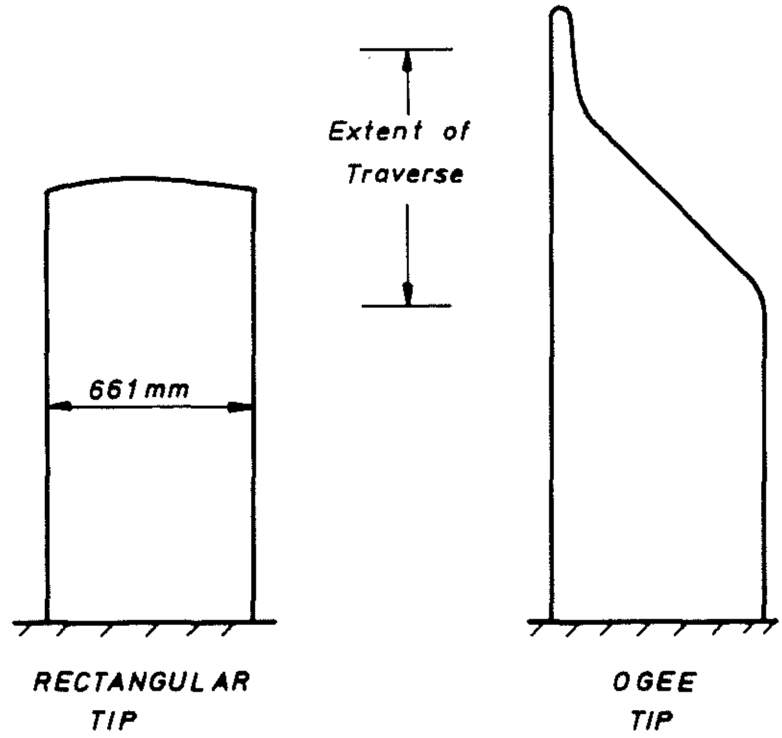

Fig 8 Half-wings studied by Rorke and Moffitt (Ref 7)

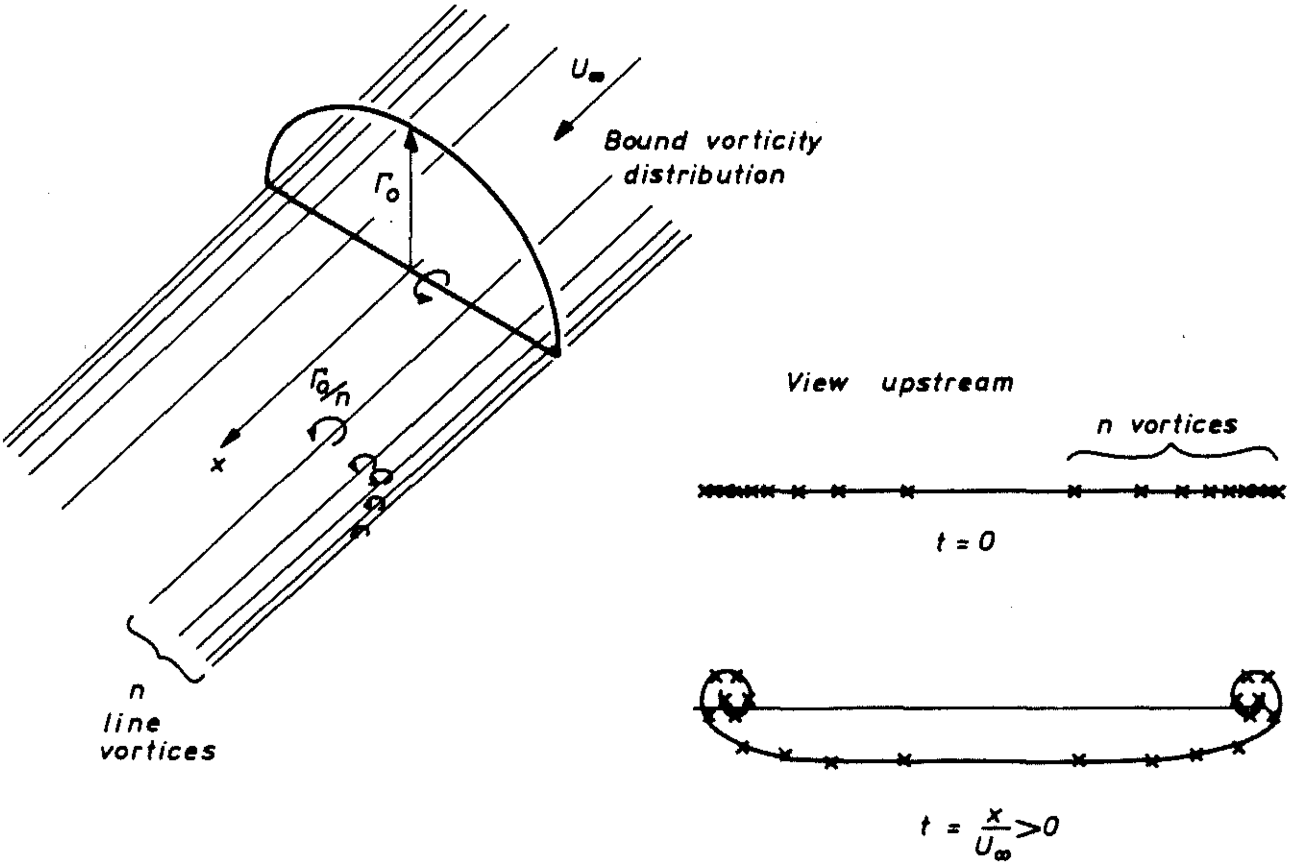

Fig 9 Line vortex model for vortex sheet roll-up

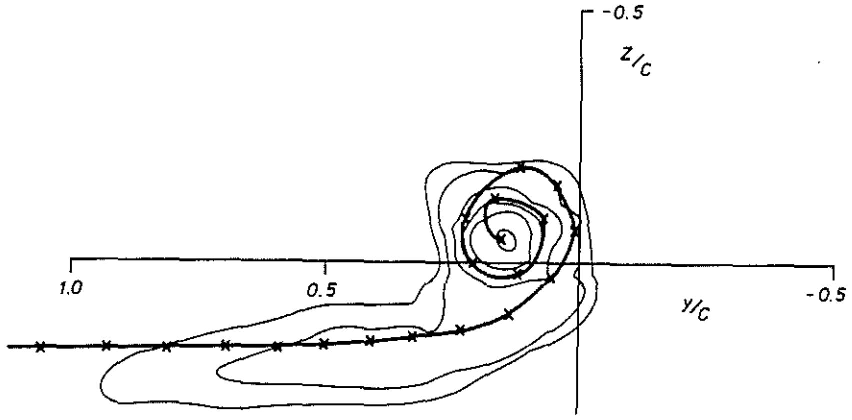

Fig 10 Vortex sheet shape predicted by line vortex model
5° incidence 25 filaments/semispan

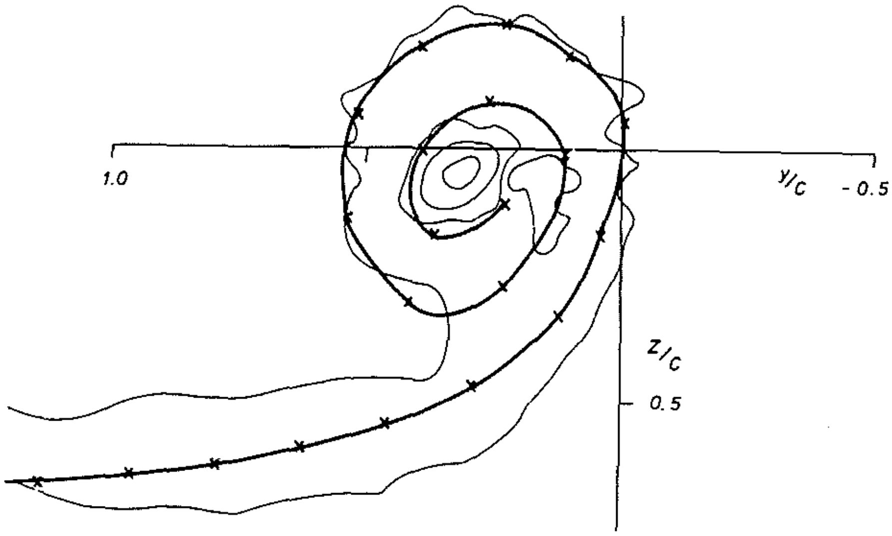

Fig 11 Vortex sheet shape predicted by line vortex model
12° incidence 25 filaments/semispan

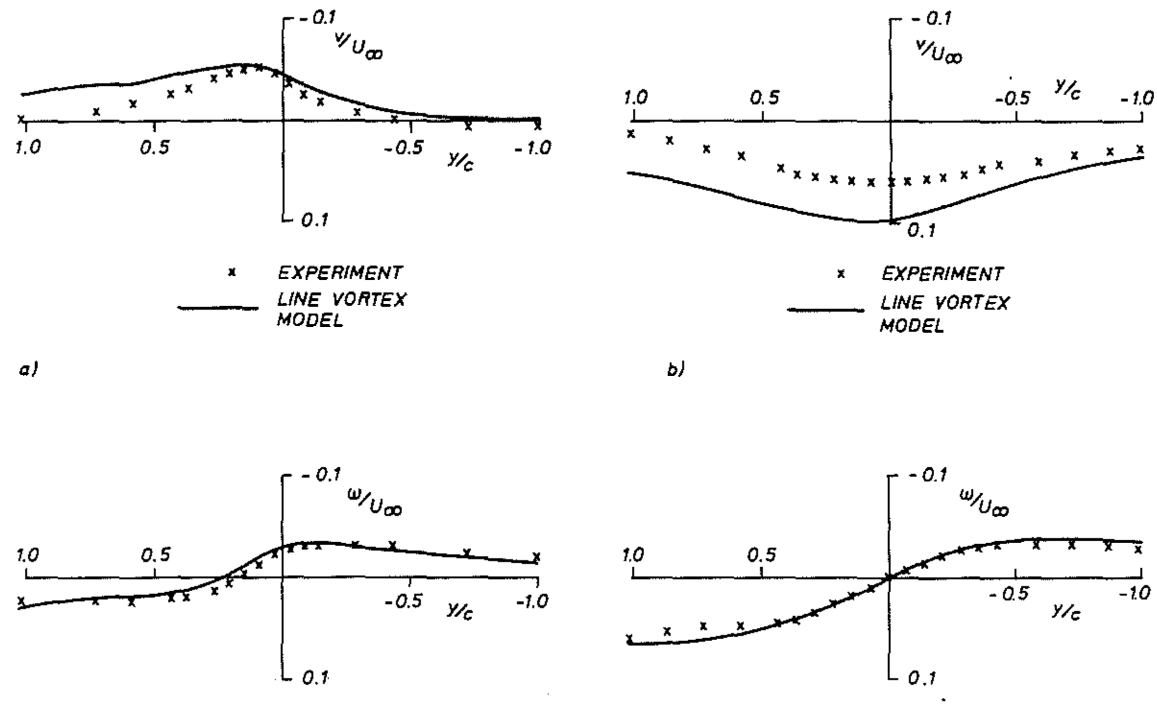

Fig 12 Experimental and theoretical velocity distributions x/c = 5.0
a) 5° incidence z/c = 0.251
b) 12° incidence z/c = -0.563

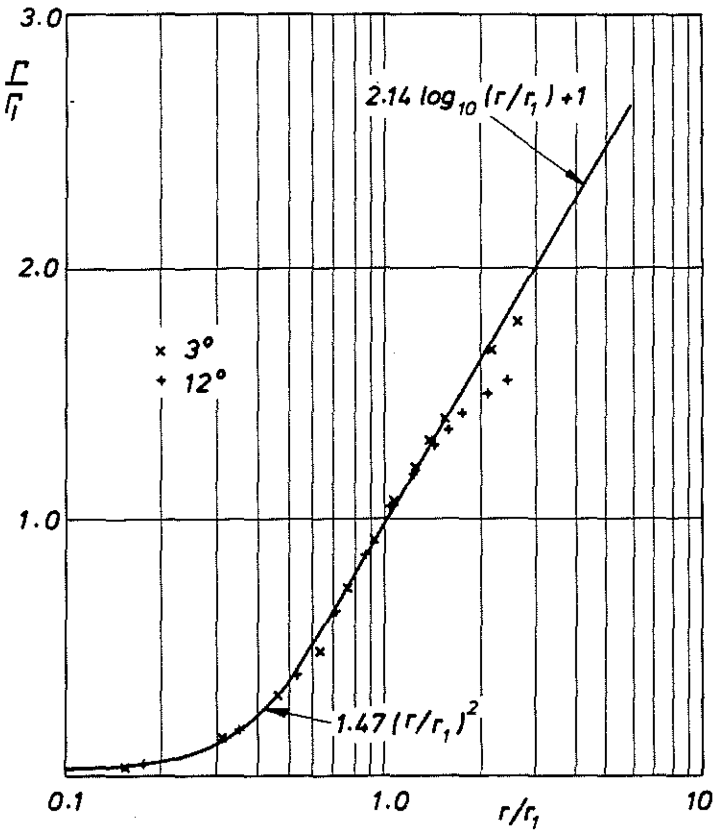

Fig 13 Circulation distributions compared with Hoffman and Joubert turbulent vortex model (Ref 11)

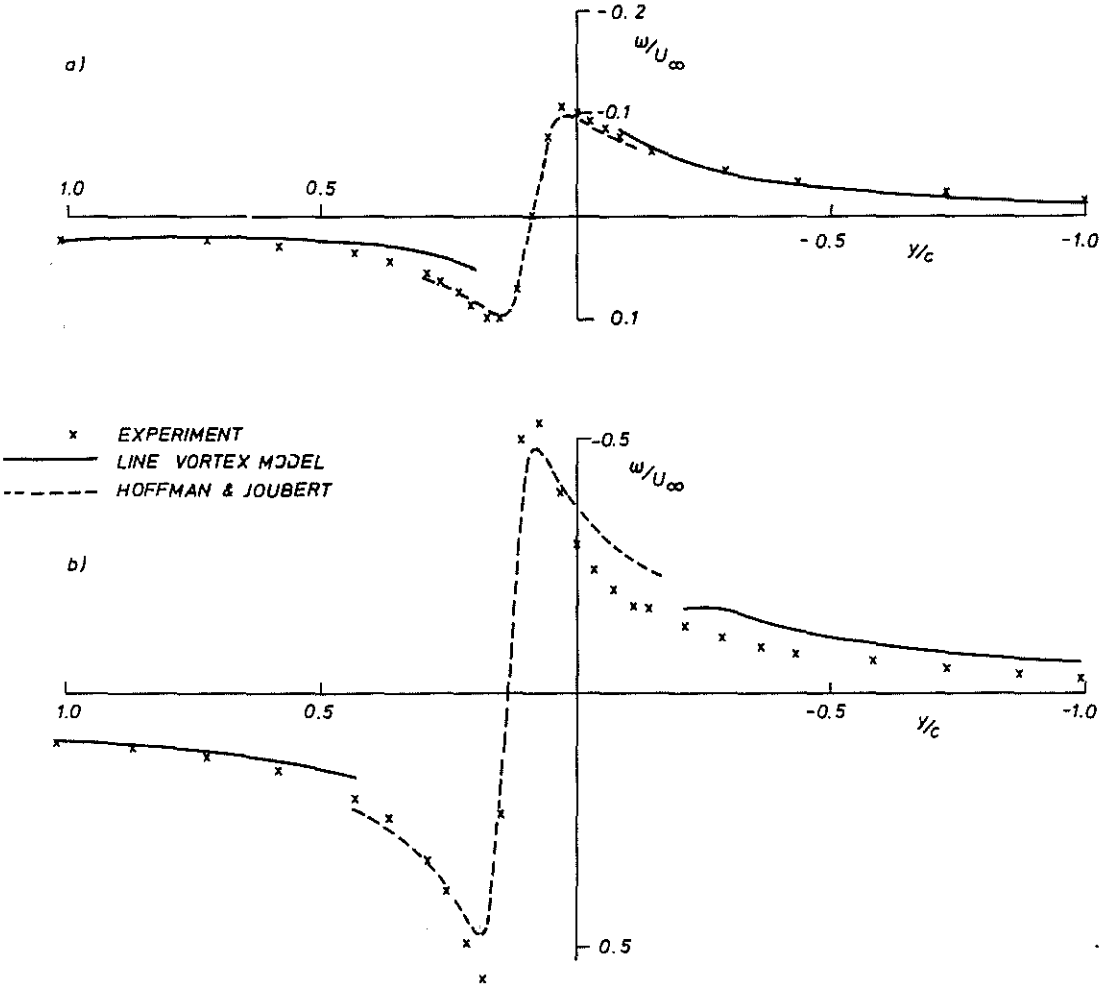

Fig 14 Experimental and theoretical velocity distributions $x/c = 5.0$
a) 3^o incidence $z/c = -0.106$
b) 12^o incidence $z/c = 0.209$